
GRAPH-BASED CLASSIFICATION OF EEG SIGNALS IN A BCI SYSTEM

Armin Navardi

Electrical Engineering Department
Sharif University of Technology
navardiarmin@gmail.com

Sepideh Hajipour Sardouie

Electrical Engineering Department
Sharif University of Technology
hajipour@sharif.edu

November 8, 2025

ABSTRACT

Graph theory is a key tool for studying behavior of the brain and different brain functions. Graph Signal Processing (GSP) is a powerful framework for analyzing graph-structured data and has gained significant recognition in data science, signal processing, machine learning, and neuroscience. In this paper, we propose a method by combining the power of Graph Signal Processing and robust machine learning methods to perform interpretable classification of EEG signals and outperform state-of-the-art methods in machine learning and Graph Signal Processing. Our framework also enables the extraction of task-related brain connectivities associated with various mental and motor imagery tasks performed by patients with neurological impairments.

1 Introduction

Brain-Computer Interface (BCI) systems have gained significant attention in recent years due to their potential applications in assistive technology, neurorehabilitation, and human-computer interaction. These systems aim to establish a direct communication pathway between the human brain and external devices by decoding brain activity, often recorded using electroencephalography (EEG). EEG signals, being non-invasive and high-temporal-resolution data sources, provide valuable insights into brain dynamics but also pose significant challenges due to their non-stationary nature, low signal-to-noise ratio, and inter-subject variability.

Traditional EEG classification methods, such as machine learning and deep learning models, rely heavily on feature extraction and handcrafted techniques to capture the discriminative characteristics of brain signals. However, these approaches often struggle with the complex connectivity patterns and spatial-temporal dependencies inherent in EEG signals. Graph-based methods have recently emerged as a powerful alternative, leveraging graph structures to model the relationships between EEG channels and enhance classification performance.

Our Contribution: In this work, we propose a method that leverages previous GSP-based algorithms by integrating discriminative graph learning for robust and interpretable graph extraction, the Fukunaga–Koontz transform for effective feature extraction, the graph Fourier transform, and non-linear classifiers. We also introduce a more suitable optimization algorithm for graph learning. In addition, we compare our method with other state-of-the-art approaches designed for scarce data.

2 Preliminaries

2.1 Graph Signal Processing

Adjacency Matrix of a Graph: In graph signal processing, an adjacency matrix is a fundamental graph representation that encodes the relationships between its nodes. Given a graph $G = (V, E)$, where V is the set of N nodes and E

is the set of edges connecting them, the adjacency matrix A is defined as an $N \times N$ matrix where each element A_{ij} represents the weight of the edge between node i and node j .

In the context of EEG signal processing, the adjacency matrix is used to represent functional or structural connectivity between EEG channels. The functional connectivities may be defined based on measures such as correlation, coherence, mutual information, or graph-theoretic distances between EEG signals. This representation allows for the application of graph-based techniques to analyze and classify EEG signals in a BCI system.

Graph Fourier Transform: The Graph Fourier Transform decomposes a graph signal into topological components. These components are the eigenvectors of the Laplacian matrix ($L = D - A$) that serve as the graph's frequency modes. Given a graph signal x and a graph G with its Laplacian eigenvectors arranged as columns of V , the graph Fourier transform of x with respect to the graph is obtained from equation 1. The eigenvectors associated with small eigenvalues are considered low-frequency modes that vary slowly across connected nodes, while large eigenvalues represent high-frequency modes with rapid variation between neighboring nodes. Notably, any graph signal could be represented as a linear combination of all the graph modes. The GFT thus reveals how a graph signal distributes across smooth and oscillatory patterns relative to the underlying topology, enabling the design of spectral filters, the study of localized versus global dynamics, and the extension of classical signal processing and machine learning techniques such as filtering, neural networks, etc. to graph-structured data [15, 1].

$$\hat{x} = V^T x \quad (1)$$

2.2 Graph Learning

One of the common approaches to learning graph from observed data is based on graph smoothness assumption. This method originates in graph signal processing and its main assumption is that the resulting graphs must be smooth with respect to the observed signals. In this context total variation of the signal x with respect to a graph g is defined as:

$$TV_g(x) = \sum A_{ij}(x_i - x_j)^2 = x^T L x \quad (2)$$

which $L = D - A$ is the Laplacian matrix of the graph. This term measures how close the neighboring nodes of the graph are. In other words, a lower total variation means that neighboring nodes have more similar values and the graph is smoother with respect to the signal. In general we have:

$$\text{tr}(X^T L X) = \frac{1}{2} \text{tr}(W Z) = \frac{1}{2} \|W \circ Z\|_{1,1} \quad (3)$$

Kalefolias introduced a general model for learning a sparse graph with no isolated vertex when no prior information is available. Later on, sabokseyr utilized this framework for learning task-specific graphs. The objective introduced by Kalefolias is eq 3. This objective contains the total variation of the graph and two regularization terms. The logarithmic barrier prevents two things: 1) prevents the edges from becoming negative and 2) prevents isolation of vertices. The other term forces the graph to be sparser and have fewer edges.

$$\min_{W \in \mathcal{W}_m} TV_g(X) + f_{reg}(W) = \min_{W \in \mathcal{W}_m} \|W \circ Z\|_{1,1} - \alpha \mathbf{1}^\top \log(W \mathbf{1}) + \beta \|W\|_F^2. \quad (4)$$

3 Discriminative Graph Learning

Saboseyr adopted a discriminative graph learning framework that takes task-specific information into account when learning the underlying graphs from the observed signals. In this method the goal is to learn smooth and sparse graphs for each class such that the signals of each class are smooth to its own graph and non-smooth to the graph of other classes.

3.1 Problem Formulation

Let the dataset $\mathcal{X} = \bigcup_{c=1}^C \mathcal{X}_c$ comprise labeled graph signals from C classes, where each subset $\mathcal{X}_c = \{\mathbf{x}_p^{(c)}\}_{p=1}^{P_c}$ represents signals from class c . Each class is assumed to be associated with a distinct underlying graph $\mathcal{G}_c = (\mathcal{V}, \mathcal{E}_c, \mathbf{W}_c)$, where $\mathbf{W}_c \in \mathbb{R}^{N \times N}$ is the adjacency matrix. The main assumption of this method is that the signals of each class are smooth with respect to their own graph while non-smooth to graph of the other classes.

3.2 Optimization Objective

The goal is to learn each class-specific adjacency matrix \mathbf{W}_c such that signals in class c are smooth on \mathcal{G}_c , while signals from other classes are not. To this end, the following convex optimization problem is solved for each class:

$$\min_{\mathbf{W}_c \in \mathcal{W}_m} \|\mathbf{W}_c \circ \mathbf{Z}_c\|_1 - \alpha \mathbf{1}^\top \log(\mathbf{W}_c \mathbf{1}) + \beta \|\mathbf{W}_c\|_F^2 - \gamma \sum_{k \neq c} \|\mathbf{W}_c \circ \mathbf{Z}_k\|_1, \quad (5)$$

where:

- \mathbf{W}_c is the symmetric adjacency matrix for class c , constrained to the set $\mathcal{W}_m = \{\mathbf{W} \in \mathbb{R}_+^{N \times N} \mid \mathbf{W} = \mathbf{W}^\top, \text{diag}(\mathbf{W}) = 0\}$.
- \mathbf{Z}_c is a pairwise distance matrix constructed from signals in \mathcal{X}_c .
- \circ denotes the Hadamard (elementwise) product.
- α, β , and γ are positive regularization parameters.

4 Methodology

4.1 Experimental Setup

Experimental Paradigm: The experiment consists of two sessions conducted on two different days with 9 participants who suffered from disability caused by spinal cord injury and stroke. During each session subjects performed 40 trials for each of the 5 tasks while the EEG signals were recorded. At the beginning of each trial of the experiment, a cross cue is shown to the subjects to fixate on it for relaxation and avoiding eye movement. At $t = 3$ s, a beep was sounded and one of the five cues displayed in Fig 3 appeared right after the beep and the subject had to perform the mental or motor imagery task right related to the cue until another beep was sounded at $t = 10$ s. After the inter-trial-interval (about 2.5-3.5 s), the next trial began. The cues were ordered randomly and each corresponds to a specific mental or motor imagery task described as below [13]:

- **Word Association (WORD):** Participants were instructed to generate as many words as possible starting with a given letter in Spanish. Letters were presented in a pseudo-randomized sequence.
 - **Mental Subtraction (SUB):** Participants performed successive elementary subtractions, subtracting a randomly chosen single-digit number from a randomly selected number between 15 and 30.
 - **Spatial Navigation (NAV):** Participants were asked to mentally imagine navigating through a familiar home environment, focusing on spatial orientation.
 - **Motor Imagery of the Right Hand (HAND):** Participants engaged in kinesthetic imagery of repetitively squeezing a hand-sized ball with their hand.
- Motor Imagery of Both Feet (FEET): Participants performed kinesthetic imagery of repetitive, self-paced movements of both feet without actual physical motion.

Data Acquisition The EEG data was recorded using 30 electrodes according to the international 10–20 system at a sampling rate of 256 Hz. The electrodes include channels AFz, F7, F3, Fz, F4, F8, FC3, FCz, FC4, T3, C3, Cz, C4, T4, CP3, CPz, CP4, P7, P5, P3, P1, Pz, P2, P4, P6, P8, PO3, PO4, O1, and O2. For recording the signals, the g.tec GAMMAsys system with g.LADYbird active electrodes and two g.USBamp biosignal amplifiers (Guger Technologies, Graz, Austria) was used. In addition, the EEG signals were filtered using a notch filter and a band pass filter with 0.5 and 100 Hz cutoff frequencies [13].

4.2 Data Preprocessing

We only used data from 4 subjects, since the performance of other subjects and the data acquired from them was extremely poor [13]. For enhancement of signals, we first normalized the EEG channels by their variance. Subsequently, the trials were extracted by cropping signals from 4.5 to 7.5 s after each trial start. In order to show our robustness of our method, no further processing, filtering, or trial removal was performed.

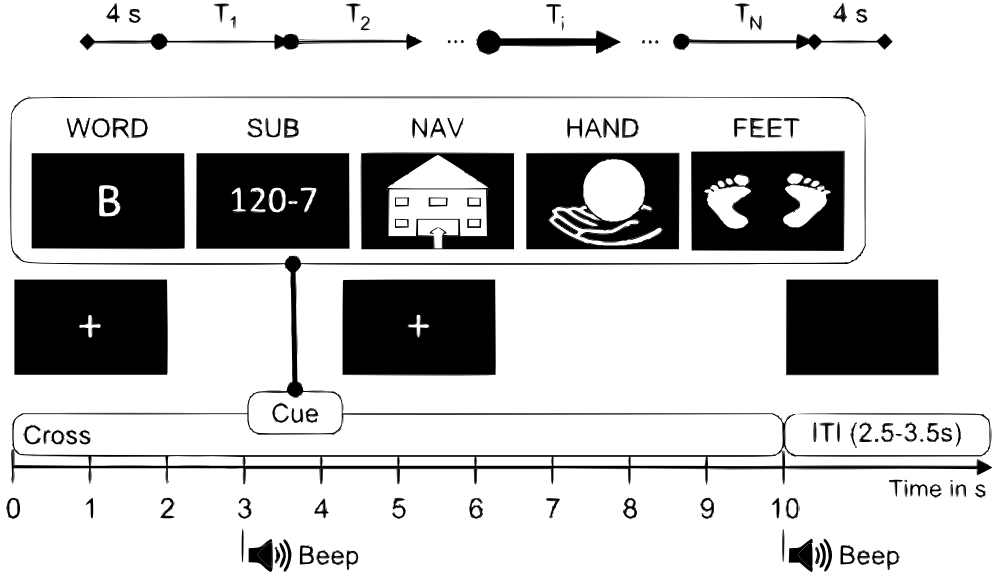


Figure 1: Experimental paradigm

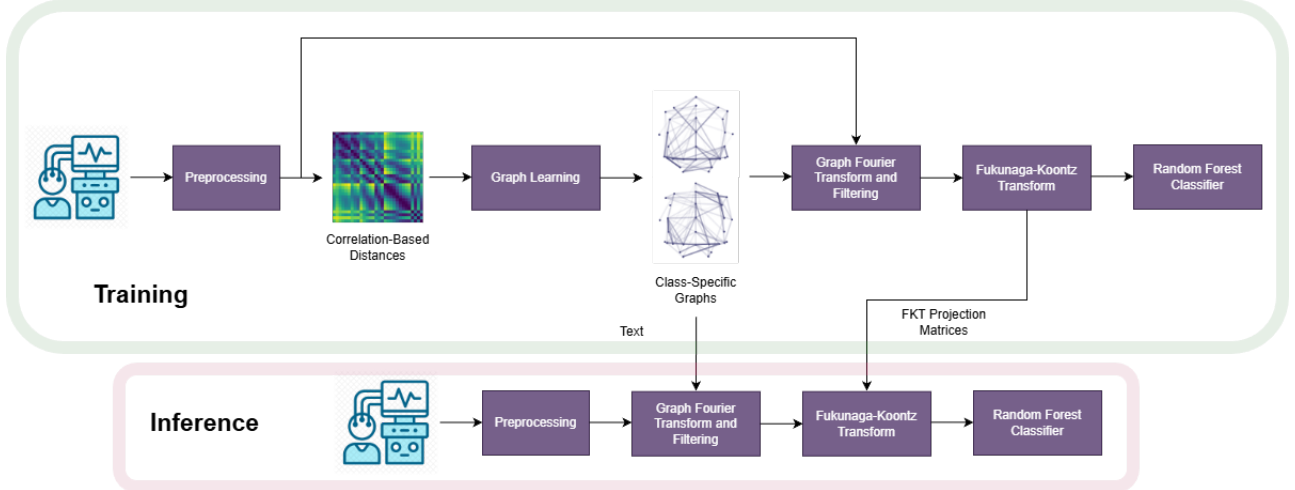


Figure 2: Overall flow of our proposed method

4.3 Proposed Method

Learning Class-Specific Graphs The first step in our method is to learn class-specific graphs using Discriminative Graph Learning. The reason for choosing this graph learning algorithm is its ability to focus on task-related brain networks and maintain more informative features. To run this algorithm, we calculate channel-wise distance matrices corresponding to each class (\tilde{W}_c) and pass the distance matrices to the graph learning algorithm in eq 5. Additionally, we used a correlation-based distance metric as an alternative to Euclidean distance. This is because EEG channels have different scales and artifacts that make the Euclidean distance unsuitable.

Optimization Algorithm: We simply prove that the objective in eq 5 could be transformed into the objective 7 by introducing a new variable \tilde{X} . In this manner, we simply use the algorithm proposed by Kalefolias to learn a graph for each class. Additionally, this format makes us able to use better measures of distance such as correlation making it suitable for cases with inconsistent channel scales.

$$\tilde{X}_c = [X_c, i\sqrt{\gamma}X_1, i\sqrt{\gamma}X_2, \dots] \quad (6)$$

$$\begin{aligned}
& \Rightarrow \frac{1}{2} \|\tilde{\mathbf{W}}_c \circ \tilde{\mathbf{Z}}_c\|_1 = \text{trace}(\tilde{X}_c^T L_c \tilde{X}_c) = \text{trace}\left(\begin{bmatrix} X_c^T \\ i\sqrt{\gamma}X_1^T \\ \vdots \end{bmatrix} L_c \begin{bmatrix} X_c & i\sqrt{\gamma}X_1 & \dots \end{bmatrix}\right) \\
& = \text{trace}\left(\begin{bmatrix} X_c^T L_c X_c & i\sqrt{\gamma}X_c^T L_c X_1 & \dots & i\sqrt{\gamma}X_c^T L_c X_N \\ i\sqrt{\gamma}X_1^T L_c X_c & -\gamma X_1^T L_c X_1 & \dots & -\gamma X_1^T L_c X_N \\ \vdots & \vdots & \ddots & \vdots \\ i\sqrt{\gamma}X_N^T L_c X_c & -\gamma X_N^T L_c X_1 & \dots & -\gamma X_N^T L_c X_N \end{bmatrix}\right) \\
& = \text{trace}(X_c^T L_c X_c) - \gamma \sum_{k \neq c} \text{trace}(X_k^T L_c X_k) = \frac{1}{2} \|\mathbf{W}_c \circ \mathbf{Z}_c\|_1 - \frac{\gamma}{2} \sum_{k \neq c} \|\mathbf{W}_c \circ \mathbf{Z}_k\|_1 \\
& \min_{\tilde{W}_c \in \mathcal{W}_m} \|\tilde{W}_c \circ \tilde{Z}_c\|_{1,1} - \alpha \mathbf{1}^\top \log(\tilde{W}_c \mathbf{1}) + \beta \|\tilde{W}_c\|_F^2. \quad (7)
\end{aligned}$$

Graph Fourier Filtering Subsequently, we transform the EEG signals from channel domain to graph Fourier domain. The graph Fourier transform reveals insights into how brain regions interact over time and how different graph modes are combined at each moment. More specifically, each GFT coefficient is the projection of the graph signal onto one Laplacian eigenvector and tells you how much of that graph frequency mode is present in the signal, just like Fourier coefficients tell you how much of each sinusoid is present in a time signal. [15] Since Laplacian eigenvectors corresponding to lower eigenvalues are low-frequency modes of the graph, these eigenvectors indicate smooth modes of the graph. In other words, lower-frequency graph modes, associated with small Laplacian eigenvalues, correspond to smooth patterns that are spread across the brain and often align with large-scale sub-networks. In contrast, higher-frequency modes, associated with larger eigenvalues, capture localized variations with strong differences between neighboring brain regions. [15] [16] Therefore, we only keep first N_{gft} frequencies of the graph which is equivalent to applying a low-pass filter in the graph Fourier domain.

$$\hat{X}_{filtered} = V_{1:N_{gft}}^T X \quad (8)$$

Finding a Discriminative Subspace Through FKT and Classification The next step is to find a subspace in which the data of different classes are highly discriminated. This is done by applying a Fukunaga-Koontz transform on the graph filtered signals. The projection weights of the FKT algorithm are the solutions of the generalized eigenvalue problem in eq 9 which is finding weights that maximize generalized Rayleigh quotient between two covariance matrices S_i and S_j calculated from the graph-Fourier domain filtered signals of class i and j . Therefore, by calculating variance of the resulting matrix along the time dimension, we get greatly informative features for classification. Lastly, we train a random forest classifier on these features and perform classification. This procedure allows us to exploit the strength of Graph-Signal Processing and highly non-linear classifiers. Since the data acquired for each subject is too scarce and noisy, we performed 10-fold cross validation and calculated average validation accuracy of each fold to better make use of the available data. Additionally, we implemented and performed other algorithms used previously and compared them with our method [2] [14]. The overall workflow of our method is illustrated in Fig. 2.

$$w = \text{argmax} \frac{w^T S_i w}{w^T S_j w} \quad (9)$$

Table 1: Classification Accuracies

Subject	Class	Accuracy (%)		
		Our Method	Structural	CSP
Subject F	WORD vs HAND	80.00	80.00	68.75
	SUB vs NAV	90.00	86.25	95.00
	NAV vs HAND	90.00	87.50	85.00
	SUB vs HAND	85.00	82.50	85.00
	SUB vs FEET	90.00	88.75	87.50
	WORD vs FEET	73.75	72.50	68.75
	NAV vs FEET	67.50	67.50	65.00
	WORD vs SUB	86.25	78.75	87.50
	WORD vs NAV	86.25	80.00	78.75
Subject D	HAND vs FEET	81.25	76.25	73.75
	WORD vs HAND	76.25	70.00	70.00
	SUB vs NAV	85.00	81.25	77.50
	NAV vs HAND	80.00	83.75	82.50
	SUB vs HAND	78.75	73.75	70.00
	SUB vs FEET	70.00	73.75	70.00
	WORD vs FEET	86.25	80.00	76.25
	NAV vs FEET	75.00	78.75	83.75
	WORD vs SUB	73.75	70.00	70.00
Subject E	WORD vs NAV	86.25	81.25	93.75
	HAND vs FEET	67.50	61.25	52.50
	WORD vs HAND	85.00	80.00	76.25
	SUB vs NAV	76.25	73.75	67.50
	NAV vs HAND	81.25	77.50	75.00
	SUB vs HAND	78.75	72.50	68.75
	SUB vs FEET	73.75	76.25	76.25
	WORD vs FEET	81.25	80.00	81.25
	NAV vs FEET	78.75	75.00	76.25

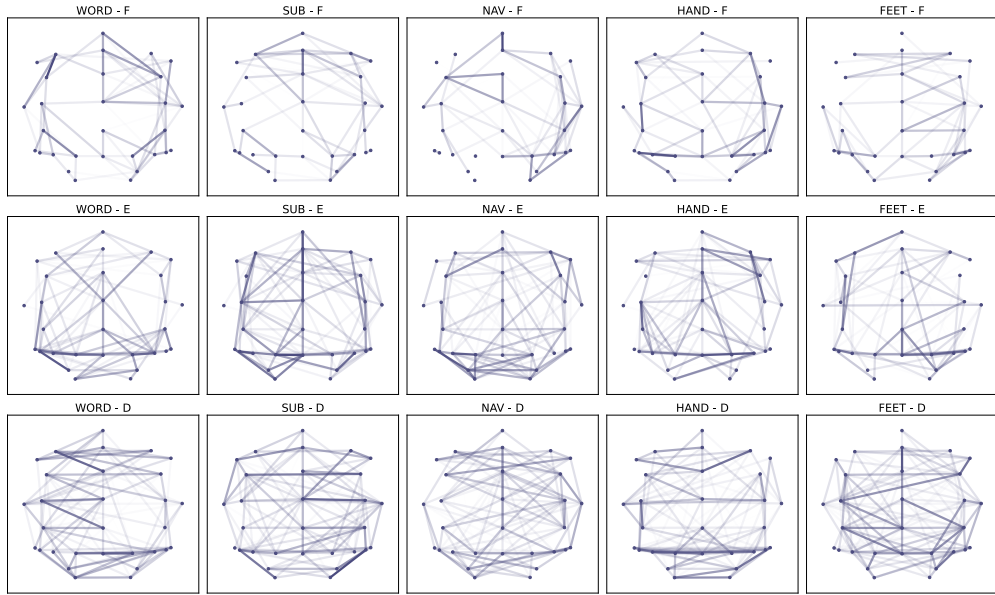
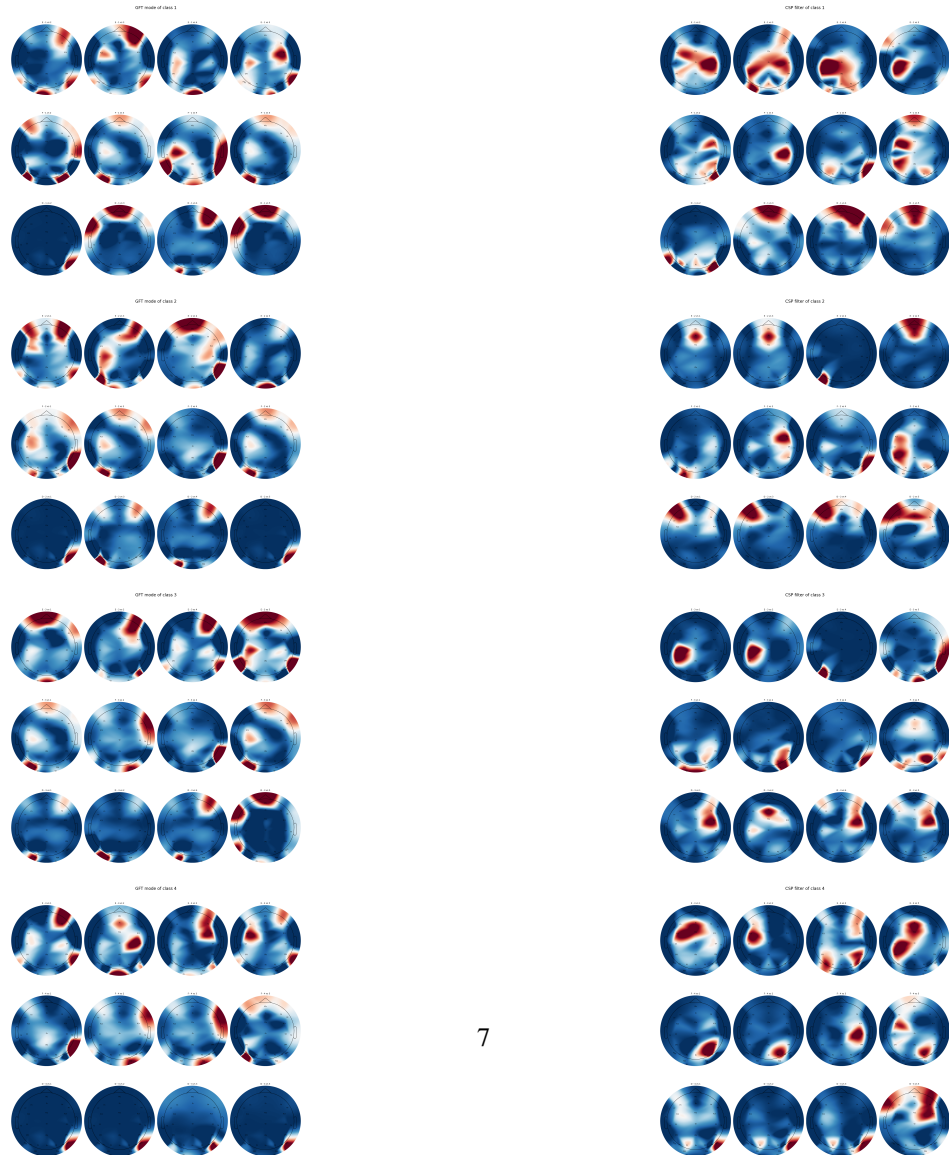


Figure 3: Overall flow of our proposed method

5 Results



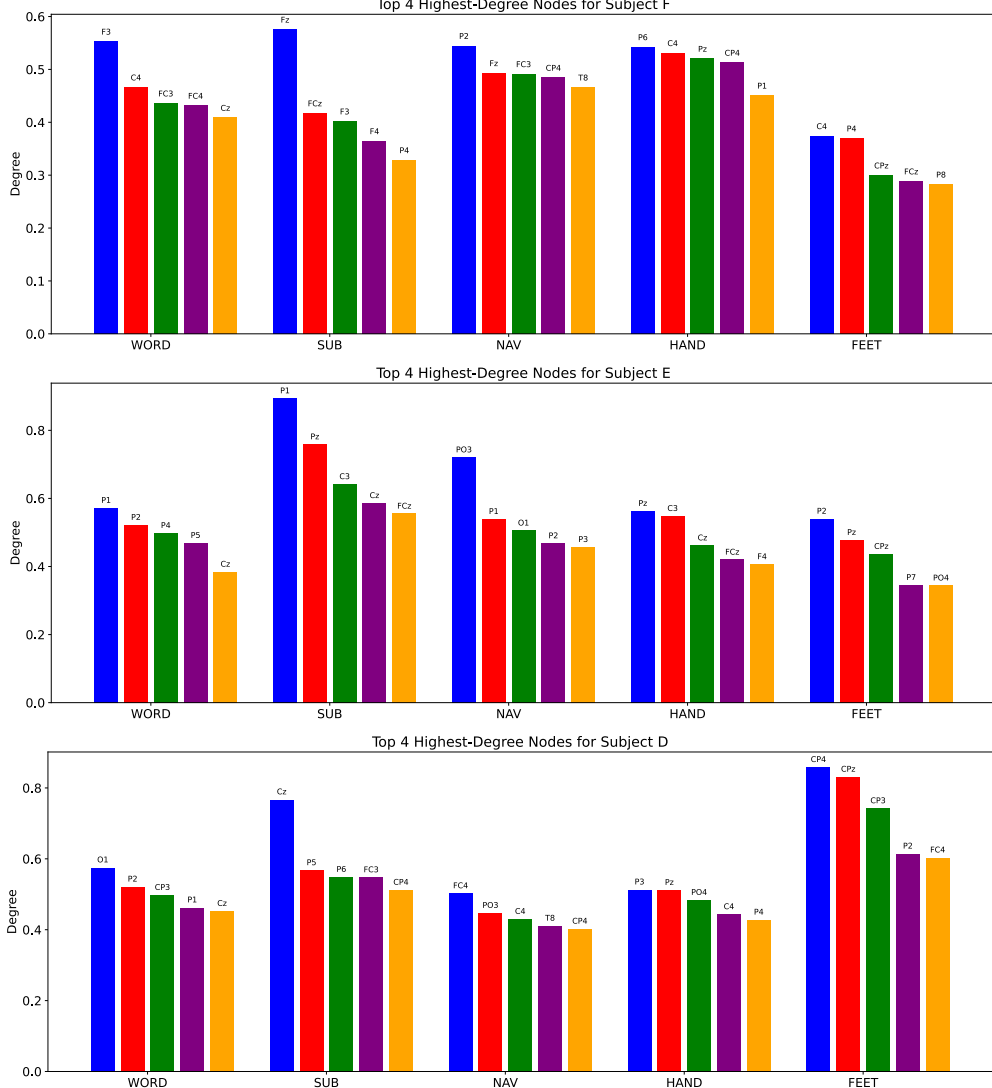


Figure 4: Top node degrees of the obtained graphs for each subject

5.1 Comparison with other methods

The cross-validation accuracies for different methods are presented in Table 1. The results indicate that our method improves average classification accuracy for all subjects and performs better for most of the classification pairs. Additionally, our method performs consistently and has less variation across different classification pairs while performance of other methods vary significantly. Additionally, we obtained the graph mode with highest discrimination for each pair and subject as well as the first CSP filter for each pair and subject. Fig. 5 and 6 illustrate the graph modes and the csp filters. The graph modes and the csp filters have overlapping brain regions in most of the pairs while the CSP filters are more localized and isolated, the graph modes have more complex patterns for most of the pairs. Notably, the patterns vary significantly across subjects for some of the pairs since the subjects have brain and spinal cord injuries.

5.2 Obtained Graphs

The analysis of the three subjects with neurological impairments revealed consistent yet individually variable connectivity patterns (Fig. 3, 4) across the five motor and cognitive tasks (WORD, SUB, NAV, HAND, and FEET). In all subjects, the electrodes with the highest network degree corresponded well with regions typically associated with task-specific neural processing. For instance, the WORD task elicited strong connection over frontal and fronto-central electrodes (e.g., F3, FC3, FC4), reflecting engagement of the left-lateralized language and semantic processing networks

[17, 18]. The SUB task showed prominent activity in midline frontal sites (e.g., Fz, FCz, Cz), which aligns with the expected involvement of the dorsolateral prefrontal cortex and anterior cingulate during arithmetic reasoning and working memory operations [19, 20]. The NAV condition produced high-degree nodes in parietal and occipital regions (e.g., P2, P3, PO3), supporting the recruitment of visuospatial and parietal cortical networks responsible for spatial orientation and attention [21]. For the HAND and FEET motor imagery tasks, increased connectivity was observed around central and paracentral electrodes (e.g., C4, CP4, Pz for HAND; Cz, CPz, FCz for FEET), corresponding to the somatotopic representation of limbs within the sensorimotor cortex [22, 23]. These results collectively indicate that despite the presence of cortical reorganization following stroke or spinal cord injury, the functional topography of task-related EEG connectivity largely preserves canonical motor and cognitive spatial patterns, suggesting partial maintenance of cortical specialization [24, 25].

6 Conclusion and Future Work

In this work, we developed a new algorithm to improve classification of EEG signals for disabled patients by utilizing graph signal processing and graph learning. We reformulated the multi-class graph learning algorithm and compared our method with existing algorithms. Although Graph Neural Networks need a large amount of data to perform properly and achieve considerable success on small datasets, several methods can be used to help tackle this challenge. One of the most common methods are using different loss functions and learning objectives such as contrastive learning which prevents the neural networks from overfitting. Another popular method is using deep generative models to increase the amount of datapoints in the training set. Current trending deep generative models are Generative Adversarial Networks and Diffusion-Based models which can be implemented on graph neural networks and graph signals to expand neural datasets. Another disadvantage of current GCN networks is that each layer directly maps the embedding dimensions by a fully connected layer. This results in large weight matrices when using data with large feature dimensions such as EEG signals. To tackle this challenge, one solution is using convolutional layers to map the embedding dimensions to significantly reduce the number of parameters in the network.

References

- [1] A. Ortega, P. Frossard, J. Kovačević, J. M. F. Moura, and P. Vandergheynst, “Graph signal processing: Overview, challenges, and applications,” *Proceedings of the IEEE*, vol. 106, no. 5, pp. 808–828, 2018.
- [2] S. Itani and D. Thanou, “A Graph Signal Processing Framework for the Classification of Temporal Brain Data,” 2020 28th European Signal Processing Conference (EUSIPCO), Amsterdam, Netherlands, 2021, pp. 1180-1184, doi: 10.23919/Eusipco47968.2020.9287486. keywords: Autism;Signal processing algorithms;Signal processing;Tools;Prediction algorithms;Topology;Classification algorithms;Graph signal processing;machine learning;explainability;decision trees;functional MRI;autism spectrum disorder,
- [3] Fukunaga, K., and Koontz, W. L. G. (1970). *Application of the Karhunen–Loève expansion to feature selection and ordering*. IEEE Transactions on Computers, C-19(4), 311–318.
- [4] How to learn a graph from smooth signals
- [5] George Kour and Raid Saabne. Real-time segmentation of on-line handwritten arabic script. In *Frontiers in Handwriting Recognition (ICFHR), 2014 14th International Conference on*, pages 417–422. IEEE, 2014.
- [6] George Kour and Raid Saabne. Fast classification of handwritten on-line arabic characters. In *Soft Computing and Pattern Recognition (SoCPaR), 2014 6th International Conference of*, pages 312–318. IEEE, 2014.
- [7] Guy Hadash, Einat Kermany, Boaz Carmeli, Ofer Lavi, George Kour, and Alon Jacovi. Estimate and replace: A novel approach to integrating deep neural networks with existing applications. *arXiv preprint arXiv:1804.09028*, 2018.
- [8] X. Dong, D. Thanou, P. Frossard, and P. Vandergheynst, “Learning Laplacian matrix in smooth graph signal representations,” *IEEE Transactions on Signal Processing*, vol. 64, no. 23, pp. 6160–6173, 2016.
- [9] B. Pasdeloup, V. Gripon, G. Mercier, D. Pastor, and M. G. Rabbat, “Characterization and inference of graph diffusion processes from observations of stationary signals,” *IEEE Transactions on Signal and Information Processing over Networks*, vol. 4, no. 3, pp. 481–496, 2017.
- [10] H. Huang, Y. Wang, and L. Wang, “Graph learning based classification via multiple subspace analysis,” *IEEE Transactions on Signal Processing*, vol. 64, no. 20, pp. 5309–5321, 2016.
- [11] R. A. Fisher, “The use of multiple measurements in taxonomic problems,” *Annals of Eugenics*, vol. 7, no. 2, pp. 179–188, 1936.

- [12] M. Belkin and P. Niyogi, “Laplacian eigenmaps for dimensionality reduction and data representation,” *Neural Computation*, vol. 15, no. 6, pp. 1373–1396, 2003.
- [13] Scherer R, Faller J, Friedrich EV, Opisso E, Costa U, Kübler A, Müller-Putz GR. Individually adapted imagery improves brain-computer interface performance in end-users with disability. *PLoS One*. 2015 May 18;10(5):e0123727. doi: 10.1371/journal.pone.0123727. PMID: 25992718; PMCID: PMC4436356.
- [14] Saboksayr Seyed, Mateos. Gonzalo, Cetin Mujdat. (2021). EEG-Based Emotion Classification Using Graph Signal Processing. 1065-1069. 10.1109/ICASSP39728.2021.9414342.
- [15] D. I. Shuman, S. K. Narang, P. Frossard, A. Ortega, and P. Vandergheynst, “The emerging field of signal processing on graphs: Extending high-dimensional data analysis to networks and other irregular domains,” *IEEE Signal Processing Magazine*, vol. 30, no. 3, pp. 83–98, 2013.
- [16] S. Atasoy, I. Donner, A. S. Fries, J. D. He, E. P. Van de Ville, and J. Pearl, “Human brain networks function in connectome-specific harmonic waves,” *Nature Communications*, vol. 7, article 10340, 2016.
- [17] Julius Fridriksson et al. The functional anatomy of speech processing: from auditory cortex to motor regions. *Nature Reviews Neuroscience*, 19(11):697–708, 2018.
- [18] Cathy J. Price. A review and synthesis of the neural bases of reading and word recognition. *Neuroimage*, 62(2):816–825, 2012.
- [19] Stanislas Dehaene et al. The neural basis of arithmetic: A review and functional imaging studies. *Cognition*, 88(1):1–48, 2003.
- [20] Marie Arsalidou and Margot J. Taylor. Brain areas involved in mathematical calculations: A meta-analysis of fMRI studies in adults. *NeuroImage*, 54(4):350–367, 2011.
- [21] Russell A. Epstein. The neural basis of scene perception in humans. *Annual Review of Neuroscience*, 31:385–405, 2008.
- [22] G. Pfurtscheller and F. H. Lopes da Silva. Event-related synchronization (ERS) in the alpha band—an electrophysiological correlate of cortical idling: a review. *International Journal of Psychophysiology*, 24(1–2):39–46, 1997.
- [23] Kai J. Miller et al. Human motor cortical activity is selectively phase-entrained on underlying rhythms. *PLoS Computational Biology*, 6(9):e1000957, 2010.
- [24] Ethan R. Buch et al. Reorganization of the human ipsilesional premotor cortex after stroke. *Brain*, 135(4):1217–1229, 2012.
- [25] Martin Lotze and Leonardo G. Cohen. Motor learning and recovery after stroke: a review of imaging studies. *Progress in Neurobiology*, 72(6):349–368, 2006.